Journal of Solid Mechanics Vol. 5, No. 1 (2013) pp. 63-73

A Semi-analytical Approach to Elastic-plastic Stress Analysis of FGM Pressure Vessels

A.T. Kalali, S. Hadidi-Moud*

Mechanical Engineering Department, Ferdowsi University of Mashhad, Iran

Received 27 January 2013; accepted 23 March 2013

ABSTRACT

An analytical method for predicting elastic–plastic stress distribution in a cylindrical pressure vessel has been presented. The vessel material was a ceramic/metal functionally graded material, i.e. a particle–reinforcement composite. It was assumed that the material's plastic deformation follows an isotropic strain-hardening rule based on the von-Mises yield criterion, and that the vessel was under plane-stress conditions. The mechanical properties of the graded layer were modelled by the modified rule of mixtures. By assuming small strains, Hencky's stress–strain relation was used to obtain the governing differential equations for the plastic region. A numerical method for solving those differential equations was then proposed that enabled the prediction of stress state within the structure. Selected finite element results were also presented to establish supporting evidence for the validation of the proposed analytical modelling approach. Similar analyses were performed and solutions for spherical pressure made of FGMs were also provided.

Keywords: Functionally graded material; Elastic–plastic analysis; Pressure vessel; Modified rule of mixtures

1 INTRODUCTION

THE intensity of stress concentrations and stress effects due to the large mismatch in material properties can be substantially reduced if the microstructure transition behaviour is graded. Advances in material synthesis technologies have spurred the development of functionally graded materials (FGM) with promising applications in aerospace, transportation, energy, cutting tools, electronics, and biomedical engineering [1]. An FGM comprises a multi-phase material with volume fractions of the constituents varying gradually in a pre-determined profile, thus yielding a non-uniform microstructure in the material with continuously graded properties [2].

Elastic and elastic-plastic analyses of thick-walled pressure vessels have always attracted a lot of research interest because of their importance in engineering applications. Figueiredo et al. [3] proposed a numerical methodology in order to predict the elastic-plastic stress behaviour of functionally graded cylindrical vessels subjected to internal pressure. They assumed that the structure undergoes small strain and that the material properties of the graded layer were modeled by the modified rule of mixtures approximation. Furthermore, the plastic domain for ductile phases was defined through the Von-Mises yield criterion. They proposed an iterative method for solving the nonlinear system, combining a finite element approximation and an incremental-iterative scheme. Haghpanah et al. [4-5] extended the Variable Material Property (VMP) method developed by Jahed and Dubey [6] for materials with varying elastic and plastic properties. In the VMP method, the linear elastic solution of a boundary value problem is used as a basis to generate the inelastic solution. Through iterative analysis, the VMP

* Corresponding author.
E-mail address: hadidi@um.ac.ir (S. Hadidi-Moud).

method was used to obtain the distribution of material parameters which were considered as field variables. The application of the VMP method, generally applied to homogeneous elastic-plastic materials was extended to materials with varying elastic-plastic properties in order to calculate the residual stresses in an autofrettaged FGM cylindrical vessel by Jahed and coworkers [7-9].

Although there are several papers in the elastic analysis of FGM spherical pressure vessels in the literature [10-12], elastic-plastic stress analysis of FGM spherical pressure vessel not such a customary study. Sadeghian and ekhteraei [13] studied the thermal stress analysis for an FGM spherical pressure vessel made of Elastic–Perfectly Plastic and power law material model.

In this paper, a new analytical method is proposed for predicting stress components of a strain-hardening cylinder based on the von-Mises yield criterion under plane-stress conditions by assuming an isotropic material model. Results obtained from finite element analyses using the commercial software, ABAQUS (v 6.10), were also used to validate the proposed analytical method. The method was further extended to obtain solutions for FGM spherical vessels.

Elastic-plastic governing equations for the functionally graded cylindrical pressure vessel are presented in the next section. Section 3 describes the material properties of the graded layer modelled by the modified rule of mixtures approximation. Solution procedures and results of the elastic-plastic analysis for the FGM cylindrical vessel are presented in section 4, whereas section 5 provides key conclusions.

2 GOVERNING EQUATIONS FOR CASE STUDIES

2.1 Cylindrical pressure vessel

Consider the axisymmetric problem of a hollow circular cylinder subjected to uniform pressure on the inner surfaces. The problem can be studied in polar coordinates (r, θ). Due to axisymmetric deformations, the only displacement component is $u_r = u_r(r)$, i.e. the radial displacement. The equilibrium equations with zero body force reduce to the single equation:

$$\frac{d\sigma_r}{dr} + \frac{\sigma_r - \sigma_\theta}{r} = 0 \tag{1}$$

where σ_r and σ_θ are the radial and hoop stresses respectively.

Considering the geometric relations:

$$\varepsilon_\theta = \frac{u_r}{r} \qquad \varepsilon_r = \frac{du_r}{dr} \tag{2}$$

where ε_θ and ε_r are the hoop and radial strains in terms of the radial displacement, u_r must satisfy the compatibility equation:

$$\varepsilon_r - \varepsilon_\theta = r\frac{d\varepsilon_\theta}{dr} \tag{3}$$

Considering the quasi-static plasticity and small deformations hypothesis, the total strains may be split into elastic and plastic components as follows:

$$\begin{aligned} \varepsilon_r &= \varepsilon_r{}^p + \varepsilon_r{}^e = \varepsilon_r{}^p + \frac{(\sigma_r - \nu\sigma_\theta)}{E(r)} \\ \varepsilon_\theta &= \varepsilon_\theta{}^p + \varepsilon_\theta{}^e = \varepsilon_\theta{}^p + \frac{(\sigma_\theta - \nu\sigma_r)}{E(r)} \end{aligned} \tag{4}$$

where $E(r)$ and ν are the Young modulus and the Poisson's ratio, respectively.

It is assumed that ν is constant while $E(r)$ varies with the position across the radius of the cylindrical vessel.

Substituting Eq. (4) into Eq. (3), the governing equation for the functionally graded cylindrical vessel is obtained Eq. (5). This equation shows the relationship between stress and plastic strain.

$$\varepsilon_r{}^p - \varepsilon_\theta{}^p - r\frac{d\varepsilon_\theta{}^p}{dr} = \frac{r}{E(r)}\left(\frac{d\sigma_\theta}{dr} + \frac{d\sigma_r}{dr}\right) - \frac{r}{E^2(r)}\frac{dE(r)}{dr}(\sigma_\theta - \nu\sigma_r) \tag{5}$$

Stress and plastic strain in cylindrical vessels may be obtained by solving the differential Eqs. (1) and (5) simultaneously. However, solving this system of differential equation is not possible because the number of variables (σ_r ، σ_θ ، $\varepsilon_r{}^p$ ، $\varepsilon_\theta{}^p$) is more than the number of equations. Substituting plastic strains in terms of stresses, this system of differential equation can be solved. For a von-Mises material with associated flow rule, plastic strain increment is defined as [14]:

$$d\varepsilon^p = \frac{3}{2}\frac{d\varepsilon_e{}^p}{\sigma_e}S \tag{6}$$

where $d\varepsilon_e{}^p$ is the equivalent plastic strain increment.

σ_e , the equivalent stress and S , the deviatoric stress for plane stress are defined as:

$$\sigma_e = \sqrt{\sigma^2{}_r + \sigma^2{}_\theta - \sigma_r\sigma_\theta} \tag{7}$$

$$\begin{bmatrix} S_r \\ S_\theta \\ S_z \end{bmatrix} = \begin{bmatrix} \dfrac{2\sigma_r - \sigma_\theta}{3} \\ \dfrac{2\sigma_\theta - \sigma_r}{3} \\ -\dfrac{\sigma_r + \sigma_\theta}{3} \end{bmatrix} \tag{8}$$

Assuming small strains, the plastic stress–strain relation proposed by Hencky may be written as Eq. (9), better known as "total strain theory" [15] Mendelson explained that using the total strain theory is valid for cylindrical problems and the results match well with the actual material response [16].

$$\varepsilon^p = \frac{3}{2}\frac{\varepsilon_e{}^p}{\sigma_e}S \tag{9}$$

For a linear strain hardening material , Fig. 1, equivalent stress σ_e is determined by:

$$\sigma_e = \sigma_{y0}(r) + h_p(r)\ \varepsilon_e{}^p \tag{10}$$

and the equivalent plastic strain is obtained from:

$$\varepsilon_e{}^p = \frac{\sigma_e - \sigma_{y0}(r)}{h_p(r)} \tag{11}$$

where $h_p(r)$ is plasticity modulus (gradient of the stress–plastic strain curve) and $\sigma_{y0}(r)$ is the initial yield stress of FGM material. Both $h_p(r)$ and $\sigma_{y0}(r)$ are functions dependent on the position, r .

The plastic strain components can be determined by substituting Eqs. (7), (8), and (11) into Eq. (9):

$$\begin{bmatrix}\varepsilon_r{}^p\\ \varepsilon_\theta{}^p\\ \varepsilon_z{}^p\end{bmatrix} = \frac{3}{2}\frac{\varepsilon_e{}^p}{\sigma_e}\begin{bmatrix}S_r\\ S_\theta\\ S_z\end{bmatrix} = \frac{3}{2}\frac{\sqrt{\sigma^2{}_r+\sigma^2{}_\theta-\sigma_r\sigma_\theta}-\sigma_{y0}(r)}{h_p(r)\sqrt{\sigma^2{}_r+\sigma^2{}_\theta-\sigma_r\sigma_\theta}}\begin{bmatrix}\frac{2\sigma_r-\sigma_\theta}{3}\\ \frac{2\sigma_\theta-\sigma_r}{3}\\ -\frac{\sigma_r+\sigma_\theta}{3}\end{bmatrix} \qquad (12)$$

Furthermore, differentiating the hoop plastic strain with respect to radius (r), gives:

$$\begin{aligned}\frac{d\varepsilon_\theta{}^p}{dr} &= \frac{1}{2h_p(r)}\left(2\frac{d\sigma_\theta}{dr}-\frac{d\sigma_r}{dr}\right)\\ &-\frac{1}{2h_p{}^2(r)}(2\sigma_\theta-\sigma_r)\left(\frac{dh_p(r)}{dr}+\frac{1}{\sqrt{\sigma_\theta{}^2+\sigma_r{}^2-\sigma_r\sigma_\theta}}\left(\frac{d\sigma_{y0}(r)}{dr}h_p(r)-\frac{dh_p(r)}{dr}\sigma_{y0}(r)\right)\right)\\ &+\frac{3\sigma_{y0}(r)}{4h_p(r)\,(\sigma_\theta{}^2+\sigma_r{}^2-\sigma_r\sigma_\theta)^{\frac{3}{2}}}\left(\frac{d\sigma_r}{dr}(\sigma_\theta\sigma_r)-\frac{d\sigma_\theta}{dr}(\sigma_r{}^2)\right)\end{aligned} \qquad (13)$$

Finally, the system of differential equations (14) is obtained by substituting Eqs. (12) and (13) into Eq. (5), as:

$$\begin{cases}\dfrac{d\sigma_\theta}{dr}+\dfrac{\sigma_\theta-\sigma_r}{r}-\dfrac{1}{E(r)}\dfrac{dE(r)}{dr}(\sigma_\theta-\nu\sigma_r)=\dfrac{E(r)}{r}\dfrac{3}{2}\dfrac{\sqrt{\sigma^2{}_r+\sigma^2{}_\theta-\sigma_r\sigma_\theta}-\sigma_{y0}(r)}{h_p(r)\sqrt{\sigma^2{}_r+\sigma^2{}_\theta-\sigma_e\sigma_e}}(\sigma_r-\sigma_\theta)\\ -E(r)\left\{\dfrac{1}{2h_p(r)}\left(2\dfrac{d\sigma_\theta}{dr}-\dfrac{d\sigma_r}{dr}\right)-\dfrac{1}{2h_p{}^2(r)}(2\sigma_\theta-\sigma_r)\left(\dfrac{dh_p(r)}{dr}+\dfrac{1}{\sqrt{\sigma_\theta{}^2+\sigma_r{}^2-\sigma_r\sigma_\theta}}\left(\dfrac{d\sigma_{y0}(r)}{dr}h_p(r)-\dfrac{dh_p(r)}{dr}\sigma_{y0}(r)\right)\right)\right.\\ \left.+\dfrac{3\sigma_{y0}(r)}{4h_p(r)\,(\sigma_\theta{}^2+\sigma_r{}^2-\sigma_r\sigma_\theta)^{\frac{3}{2}}}\left(\dfrac{d\sigma_r}{dr}(\sigma_\theta\sigma_r)-\dfrac{d\sigma_\theta}{dr}(\sigma_r{}^2)\right)\right\}\\ \dfrac{d\sigma_r}{dr}=-\dfrac{\sigma_r-\sigma_\theta}{r}\end{cases} \qquad (14)$$

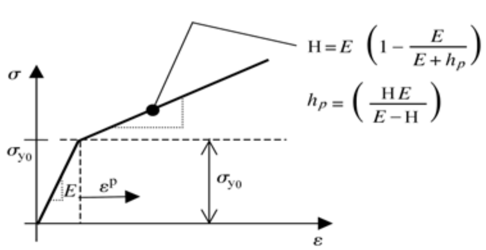

Fig. 1
Stress–strain curve for linear strain hardening.

Applying appropriate boundary conditions, distribution of radial and tangential stresses in the plastic region is obtained. We can also obtain the distribution of stress in the elastic zone from Eq. (15).

$$\begin{cases}\dfrac{d\sigma_\theta}{dr}+\dfrac{\sigma_\theta-\sigma_r}{r}=\dfrac{1}{E(r)}\dfrac{dE(r)}{dr}(\sigma_\theta-\nu\sigma_r)\\ \dfrac{d\sigma_r}{dr}=-\dfrac{\sigma_r-\sigma_\theta}{r}\end{cases} \qquad (15)$$

2.2 Spherical pressure vessel

In order to obtain stress distributions for a spherical thick-walled functionally graded pressure vessel, the equilibrium equations with zero body force reduce to the following single equation in the spherical coordinate system (r , θ , ϕ)):

$$\frac{d\sigma_r}{dr}+2\frac{\sigma_r-\sigma_\theta}{r}=0 \qquad \sigma_\theta=\sigma_\varphi \tag{16}$$

where σ_θ and σ_φ are the circumferential stresses and σ_r is the radial stress component.

Considering the geometric relations:

$$\varepsilon_\varphi=\varepsilon_\theta=\frac{u_r}{r} \qquad \varepsilon_r=\frac{du_r}{dr} \tag{17}$$

where ε_θ and ε_φ are the circumferential strains and ε_r is the radial strain in terms of the radial displacement, u_r . The compatibility equation must be satisfied:

$$\varepsilon_r-\varepsilon_\theta=r\frac{d\varepsilon_\theta}{dr} \tag{18}$$

Following similar procedures to those explained in the previous section, i.e. considering the quasi-static plasticity and small deformations hypothesis, the total strains may be split into its elastic and plastic components as follows:

$$\begin{aligned}\varepsilon_r&=\varepsilon_r{}^p+\varepsilon_r{}^e=\varepsilon_r{}^p+\frac{(\sigma_r-2\nu\sigma_\theta)}{E(r)}\\ \varepsilon_\theta\left\langle=\varepsilon_\varphi\right\rangle&=\varepsilon_\theta{}^p+\varepsilon_\theta{}^e=\varepsilon_\theta{}^p+\frac{(\sigma_\theta-\nu(\sigma_r+\sigma_\theta))}{E(r)}\end{aligned} \tag{19}$$

By substituting Eq. (19) into Eq. (18), the governing equation for the functionally graded spherical vessel is obtained Eq. (20).

$$\varepsilon_r{}^p-\varepsilon_\theta{}^p-r\frac{d\varepsilon_\theta{}^p}{dr}=\frac{r}{2E(r)}(1-\nu)(2\frac{d\sigma_\theta}{dr}+\frac{d\sigma_r}{dr})-\frac{r}{E^2(r)}\frac{dE(r)}{dr}(\sigma_\theta(1-\nu)-\nu\sigma_r) \tag{20}$$

σ_e , the equivalent stress and S , the deviatoric stress for spherical vessel are defined as:

$$\sigma_e=\frac{1}{\sqrt{2}}\sqrt{(\sigma_\theta-\sigma_\varphi)^2+(\sigma_\varphi-\sigma_r)^2+(\sigma_r-\sigma_\theta)^2}=\sigma_\theta-\sigma_r \tag{21}$$

and

$$\begin{bmatrix}S_r\\ S_\theta\\ S_\varphi\end{bmatrix}=\begin{bmatrix}-\frac{2}{3}(\sigma_\theta-\sigma_r)\\ \frac{1}{3}(\sigma_\theta-\sigma_r)\\ \frac{1}{3}(\sigma_\theta-\sigma_r)\end{bmatrix} \tag{22}$$

The plastic strain components can be determined by substituting Eqs. (21), (22), and (11) into Eq. (9):

$$\begin{bmatrix} \varepsilon_r{}^p \\ \varepsilon_\theta{}^p \\ \varepsilon_\varphi{}^p \end{bmatrix} = \frac{3}{2}\frac{\varepsilon_e{}^p}{\sigma_e}\begin{bmatrix} S_r \\ S_\theta \\ S_\varphi \end{bmatrix} = \frac{3}{2}\frac{(\sigma_\theta-\sigma_r)-\sigma_{y0}(r)}{h_p(r)\,(\sigma_\theta-\sigma_r)}\begin{bmatrix} -\frac{2}{3}(\sigma_\theta-\sigma_r) \\ \frac{1}{3}(\sigma_\theta-\sigma_r) \\ \frac{1}{3}(\sigma_\theta-\sigma_r) \end{bmatrix} = \begin{bmatrix} -\frac{1}{h_p}\left[(\sigma_\theta-\sigma_r)-\sigma_{y0}\right] \\ \frac{1}{2h_p}\left[(\sigma_\theta-\sigma_r)-\sigma_{y0}\right] \\ \frac{1}{2h_p}\left[(\sigma_\theta-\sigma_r)-\sigma_{y0}\right] \end{bmatrix} \tag{23}$$

Furthermore, differentiating the hoop plastic strain with respect to radius (r), gives:

$$\frac{d\varepsilon_\theta{}^p}{dr} = \frac{1}{2h_p{}^2(r)}\left(h_p\,(\frac{d\sigma_\theta}{dr}-\frac{d\sigma_r}{dr}-\frac{d\sigma_{y0}(r)}{dr}) - \frac{dh_p(r)}{dr}(\sigma_\theta-\sigma_r-\sigma_{y0})\right) \tag{24}$$

Finally, the system of differential Eqs. (25) is obtained by substituting Eqs. (23), and (24) into Eq. (20):

$$\begin{cases} 2\frac{d\sigma_\theta}{dr}+2\frac{\sigma_\theta-\sigma_r}{r}-\frac{1}{(1-\nu)\,E(r)}\frac{dE(r)}{dr}\left[\sigma_\theta(1-\nu)-\nu\sigma_r\right] = -\frac{E(r)}{2\,r\,(1-\nu)\,h_p(r)}\left[\sigma_\theta-\sigma_r-\sigma_{y0}(r)\right] \\ +\frac{E(r)}{2\,(1-\nu)\,h_p{}^2(r)}\left[h_p(r)(\frac{d\sigma_\theta}{dr}-\frac{d\sigma_r}{dr}-\frac{d\sigma_{y0}(r)}{dr})-\frac{dh_p(r)}{dr}(\sigma_\theta-\sigma_r-\sigma_{y0})\right] \\ \frac{d\sigma_r}{dr} = -2\frac{\sigma_r-\sigma_\theta}{r} \end{cases} \tag{25}$$

The distributions of radial and circumferential stresses in the plastic region are obtained by applying the appropriate boundary conditions. Also the distribution of stress in the elastic zone may be obtained from Eq. (26).

$$\begin{cases} \frac{d\sigma_\theta}{dr}+\frac{\sigma_\theta-\sigma_r}{r} = \frac{1}{(1-\nu)\,E(r)}\frac{dE(r)}{dr}\left[\sigma_\theta(1-\nu)-\nu\sigma_r\right] \\ \frac{d\sigma_r}{dr} = -2\,\frac{\sigma_r-\sigma_\theta}{r} \end{cases} \tag{26}$$

3 THE MECHANICAL BEHAVIOUR OF FGM

It is assumed that the functionally graded metal-ceramic composite is locally isotropic and yields according to the von Mises criterion. Three important material properties for elastic-plastic analysis are the elastic modulus $E(r)$, the initial yield stress $\sigma_{y0}(r)$, and the tangent modulus $H(r)$. These properties can be calculated using the modified rule of mixtures for composites [17].

$$E = \left[(1-f_c)\,E_m\frac{q+E_c}{q+E_m}+f_c\,E_c\right]\times\left[(1-f_c)\frac{q+E_c}{q+E_m}+f_c\right]^{-1} \tag{27}$$

$$\sigma_{y0} = \sigma_{y0m}\left[(1-f_c)+\frac{q+E_m}{q+E_c}\frac{E_c}{E_m}f_c\right] \tag{28}$$

$$H=\left[(1-f_c)H_m\frac{q+E_c}{q+H_m}+f_c E_c\right]\times\left[(1-f_c)\frac{q+E_c}{q+H_m}+f_c\right]^{-1} \tag{29}$$

$$h_p=\frac{E\,H}{E-H} \tag{30}$$

where the subscripts 'c' and 'm' indicate ceramic and metal material respectively. The volume fraction of ceramic particles is denoted by f_c, and q is the ratio of stress to strain transfer as follows, where σ_c and ε_c are the average stress and strain of ceramic respectively, and similarly for σ_m and ε_m (see Fig 2.).

$$q=\frac{\sigma_c-\sigma_m}{\left|\varepsilon_c-\varepsilon_m\right|},\quad 0<q<\infty \tag{31}$$

The empirical parameter q depends on many factors including material composition, microstructural arrangements, and the internal constraints. For example $q\to\infty$ if the constituent elements deform identically in the loading direction, while $q=0$ if the constituent elements experience the same stress level. In this analysis, the ceramic particle reinforcement is assumed to have a volume fraction that varies from 0 at the inner radius r_i, to f_{c0} at the outer radius r_o according to the following relationship:

$$f_c(r)=f_{c0}\left(\frac{r-r_i}{r_o-r_i}\right)^n \tag{32}$$

where n denotes the reinforcement distribution exponent ($n=0$ denotes uniformly-reinforced metal-ceramic).The material property for each constituent phase is listed in Table 1. The parameter q may be approximately determined by experimental calibration of tensile tests performed on monolithic composite specimens. For example, a value of $q=4.5\ Gpa$ has been used for a TiB/Ti FGM [18] whereas the Poisson ratio is constant and equal to 0.3.

Table 1
Material properties [2]

	Young's modulus (GPa)	Yield stress (MPa)	Tangent modulus (GPa)
TI	107	450	10
TIB	373		

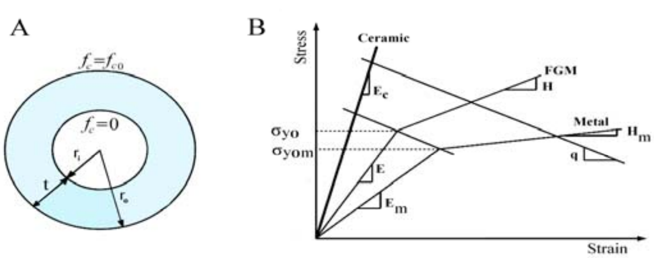

Fig. 2
(A) Schematic representation of a thick FGM vessel with internal radius r_i and external radius r_o. (B) Schematic representation of modified rule of mixtures used to estimate the behavior of ceramic particle-reinforced metal composite.

4 RESULTS

By substituting Eqs. (27)– (32) into the system of differential Eqs. (14) and (25), a set of complicated equations are obtained that are difficult to solve parametrically. Therefore, numerical methods may be used as an alternative. ODE45 Solver in MATLAB (2008) has been used for this purpose. ODE45 is a function for the numerical solution of ordinary differential equations and employs variable step size Runge-Kutta integration methods. This solver uses a 4th and 5th order pair for higher accuracy [19].

To verify the accuracy of the analytical solution, finite element analyses were performed using the commercial finite element code ABAQUS [20]. The common method for modelling FGM cylinder vessels in commercial finite element software is to subdivide the thick wall into thin layers with equal thicknesses. This method of modelling leads to a discontinuity in the mechanical properties of FGM materials and is both difficult and time-consuming. Setoodeh et al. [21] proposed a new approach for analysing the FGM material in the elastic zone without the need for division of the thickness of the cylinder into thin strips. They used the facilities available in ABAQUS software (or other commercial finite element) to define continuously variable properties. In this technique, applying a virtual temperature distribution in the cylinder wall and creating a correspondence between the distribution of temperature and mechanical properties of FGM material, allowed for variation of the FGM properties in the cylinder to be modelled. This method allowed for the analysis of the elastic-plastic FGM cylinder vessel. The three-dimensional 8-node linear coupled temperature-displacement family of finite elements in ABAQUS was used to model the cylinder. Mesh sensitivity analysis was also performed to ensure the results were not sensitive to the element size.

In order to evaluate the analytical method, a set of results from the finite element calculations obtained for the plane stress conditions were compared with results obtained from the analytical method for an FGM cylindrical vessel subjected to an internal pressure of 320 MPa (Fig.3). The results indicated that the proposed analytical method was capable of calculating stress components in a cylindrical vessel with great accuracy. The developed method was also used to study the stress components in a cylindrical FGM vessel with various ceramic particle reinforcement distributions. All the results are presented for the plane stress condition. Fig.4 illustrates the distribution of von-Mises stresses across the thickness in the cylindrical vessel subjected to different levels of internal pressure where $n = 2$ and $f_{c0} = 0.8$. The magnitude of von Mises stresses, indicate that with increasing the internal pressure, the plastically deformed region extends across the thickness of the cylinder from both the inner and the outer surfaces. In cylindrical vessels made of homogeneous material the plastic region grows only from the inner surface. Figs. 5 (A) and (B) describe the distributions of modulus of elasticity and the initial yield stress in an FGM vessel with $f_{c0} = 1$ for different reinforcement distribution exponents n. With increasing n the metal properties dominate the behaviour, overcoming the ceramic properties, and therefore the plastic behaviour of the material becomes more evident. Fig. 6 shows the von-Mises stress distribution in an FGM vessel subjected to an internal pressure of 300 MPa with $f_{c0} = 1$ and different reinforcement distribution exponents, n . By increasing n , the plastic region gradually spreads from the inner surface of the cylinder.

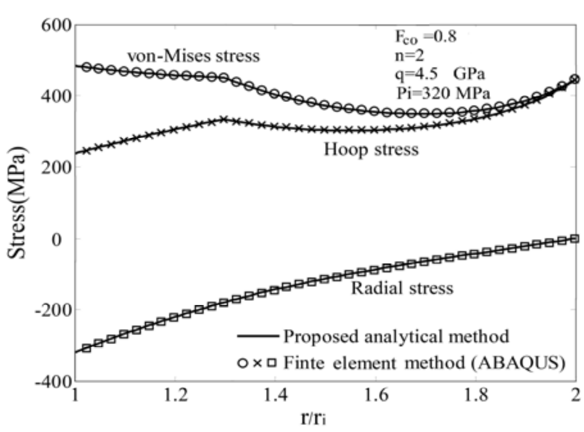

Fig. 3
Comparison with the finite element method. The results show the stress components in a cylindrical vessel with $f_{c0} = 0.8$ and $n = 2$ subjected to internal pressure $320\,\text{MPa}$. In this calculation, $q = 4.5\,\text{GPa}$. The vessel has $t/r_i = 1$ and plane-stress condition (other properties are listed in Table 1).

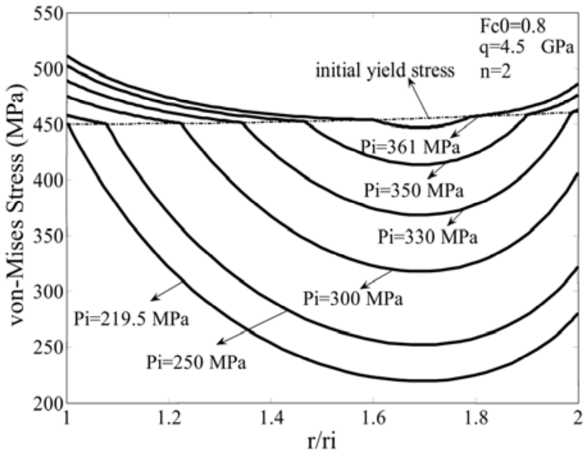

Fig. 4
von-Mises stress along the thickness in a FGM vessel subjected to different internal pressure with $f_{c0} = 0.8$ and $n = 2$. In this calculation, $q = 4.5\,\text{GPa}$. The vessel has $t/r_i = 1$ and plane-stress condition (other properties are listed in Table 1).

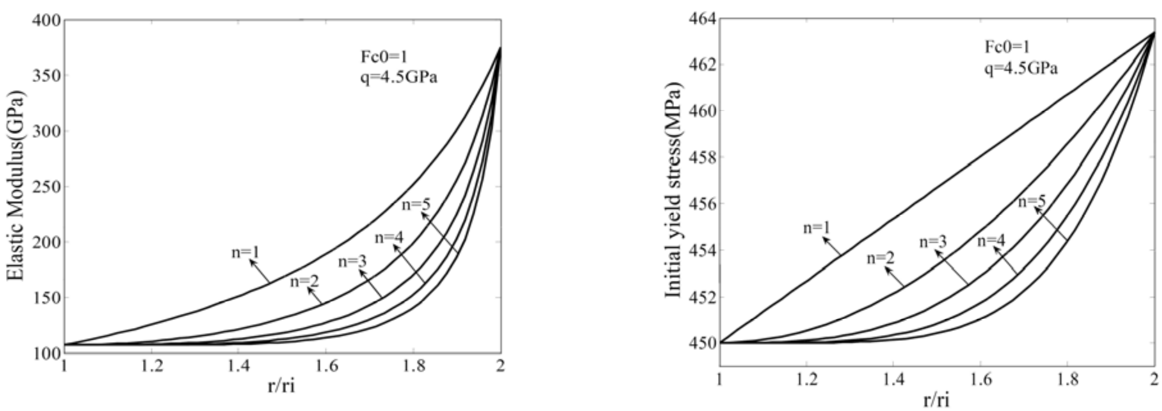

(a) (b)

Fig. 5
(A)Elasticity modulus of a FGM vessel.(B) Initial yield stress of a FGM vessel. In this set of calculations, $f_{c0} = 1$, $q = 4.5\,\text{GPa}$, $E_c = 373\,\text{GPa}$, $E_m = 107\,\text{GPa}$, $\sigma_{y0m} = 450\,\text{MPa}$ and $H_m = 10\,\text{GPa}$.

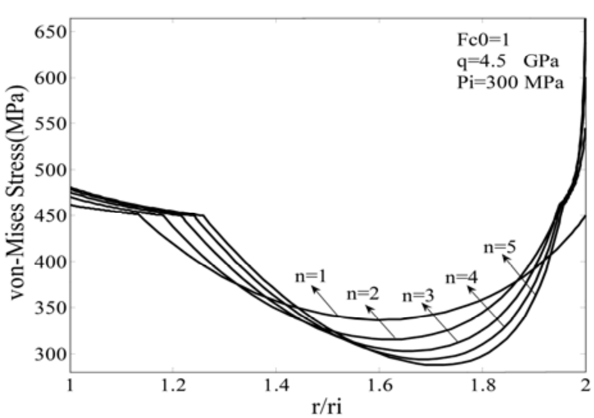

Fig. 6
von-Mises stress along the thickness in a FGM vessel subjected to internal pressure $300\,\text{MPa}$ with $f_{c0} = 1$ for different reinforcement distribution exponents, n . In this calculation, $q = 4.5\,\text{GPa}$. The vessel has $t/r_i = 1$ and plane-stress condition (other properties are listed in Table 1).

For the spherical vessel subjected to an internal pressure of 500 MPa results obtained from the analytical method were compared with the finite element analysis results. Excellent agreement was observed as shown in Fig. 7. The distribution of von Mises stresses across the thickness of the spherical vessel subjected to different levels of internal pressure is shown in Fig. 8. Similar to the case of the cylindrical vessel, with increasing internal pressure, the plastically deformed region extends across the thickness of the spherical vessel from both the inner and the outer surfaces.

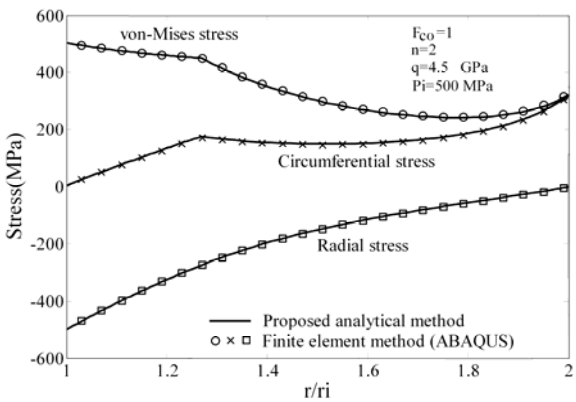

Fig. 7
Comparison with the finite element method. The results show the stress components in a spherical vessel with $f_{c0}=1$ and $n=2$ subjected to internal pressure $500\,\text{MPa}$. In this calculation, $q=4.5\,\text{GPa}$. The vessel has $t/r_i=1$ (other properties are listed in Table 1).

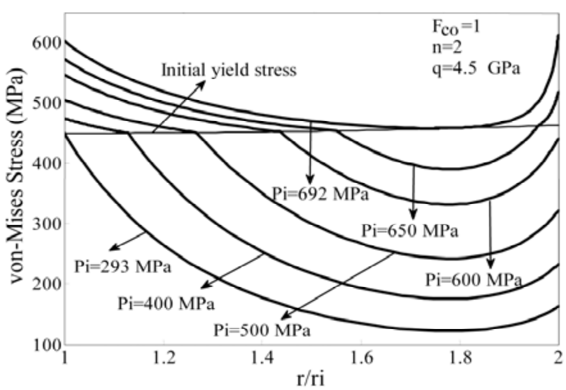

Fig. 8
von-Mises stress along the thickness in an FGM spherical vessel subjected to different internal pressure with $f_{c0}=1$ and $n=2$. In this calculation, $q=4.5\,\text{GPa}$. The vessel has $t/r_i=1$ (other properties are listed in Table 1).

5 CONCLUSION

Using a new analytical method, the elastic-plastic stress distributions in a cylindrical pressure vessels made of a FGM material were determined. Solutions previously presented for this problem were based on numerical methods such as finite element analysis [3] and the Variable Material Property (VMP) method [4, 5] whereas the technique used in this paper is based on the application of basic plasticity equations only. Despite some the limitations in the application of this method, the proposed analytical approach provided very efficient, yet accurate results for the determination of the elastic-plastic stress-strain distribution in the cylindrical pressure vessels (similarly spherical vessels) made of FGM materials.

Finite element analysis of the problem using ABAQUS commercial code was used for verification of the proposed analytical solution technique. An alternative modelling approach was developed and used for this purpose. The numerical analysis within the software was performed by the application of a "virtual thermal load" that enabled the continuous variation of material behaviour through the wall thickness of the FGM cylinder in the finite element model. An accurate solution was therefore obtained from the FE analysis. This was achieved without the need to consider a multi-layered cylinder with a stepwise solution as used in most previous solutions in the existing literature [3, 4, and 5].

The analysis results obtained in this work also indicate the possibility of formation and growth of the plastic region within the wall thickness from the external surface of the FGM vessels whereas in a cylindrical (spherical) vessels made of homogeneous materials, plasticity starts essentially from the inner surface.

REFERENCES

[1] Chakraborty A., Gopalakrishnan S., Reddy J.N., 2003, A new beam finite element for the analysis of functionally graded materials, *International Journal of Mechanical Sciences* **45**:519–539.

[2] Jin ZH., Paulino GH., Dodds Jr RH., 2003, Cohesive fracture modeling of elastic–plastic crack growth in functionally graded materials, *Engineering Fracture Mechanics* **70**:1885–912.

[3] Figueiredo F., Borges L., Rochinha F., 2008, Elasto-plastic stress analysis of thick-walled FGM pipes, *American Institute of Physics Conference Proceedings* **973**:147_52.

[4] Haghpanah Jahromi B., Farrahi GH., Maleki M., Nayeb-Hashemi H., Vaziri A., 2009, Residual stresses in autofrettaged vessel made of functionally graded material, *Engineering Structures* **31**:2930–5.

[5] Haghpanah Jahromi B., Ajdari A., Nayeb-Hashemi H., Vaziri A., 2010, Autofrettage of layered and functionally graded metal–ceramic composite vessels, *Composite Structures* **92**:1813–22.

[6] Jahed H., Dubey RN., 1997, An axisymmetric method of elastic-plastic analysis capable of predicting residual stress field, *Journal of Pressure Vessel Technology* **119**:264–73

[7] Jahed H., Farshi B., Karimi M., 2006, Optimum autofrettage and shrink-fit combination in multi-layer cylinders, *Journal of Pressure Vessel Technology* **128**:196–201.

[8] Jahed H., Farshi B., Bidabadi J., 2005, Minimum weight design of inhomogeneous rotating discs, *International Journal of Pressure Vessels and Piping* **82**:35–41.

[9] Jahed H., Shirazi R., 2001, Loading and unloading behaviour of a thermoplastic disc, *International Journal of Pressure Vessels and Piping* **78**:637–45.

[10] You LH., Zhang JJ., You XY., 2005, Elastic analysis of internally pressurized thick-walled spherical pressure vessels of functionally graded materials, *International Journal of Pressure Vessels and Piping* **82**:374–345.

[11] Dai HL., Fu YM., Dong ZM., 2006, Exact solutions for functionally graded pressure vessels in a uniform magnetic field, *International Journal of Solids and Structures* **43**:5570–80.

[12] Chen YZ., Lin XY., 2008, Elastic analysis for thick cylinders and spherical pressure vessels made of functionally graded materials, *Computational Materials Science* **44**:581–587.

[13] Sadeghian M., Ekhteraei H., 2011, Axisymmetric yielding of functionally graded spherical vessel under thermo-mechanical loading, *Computational Materials Science* **50**:975–81.

[14] Dunne F., Petrinic N., 2006, *Introduction to Computational Plasticity*, Oxford University Press.

[15] Chakrabarty J., 2006, *Theory of Plasticity*, UK, Elsevier Butterworth Heinemann, 3rd Edition.

[16] Mendelson A., 1968, *Plasticity: Theory and Application*, New York, Macmillan.

[17] Suresh S., Mortensen A., 1998, *Fundamentals of Functionally Graded Materials*, IOM Communications Ltd.

[18] Carpenter RD., Liang WW., Paulino GH., Gibeling JC., Munir ZA., 1999, Fracture testing and analysis of a layered functionally graded Ti/TiB beam in 3-point bending, *Materials Science Forum* **308–311**:837–42.

[19] Jamshidi N., Abouei A., Molaei R., Rezaei R., Jamshidi M., 2011, *Applied Guide on MATLAB*, Tehran, Abed.

[20] Karlsson., Hibbitt., Sorensen., 2008, ABAQUS/CAE, Version 6.8-1.

[21] Setoodeh A., Kalali A., Hosseini A., 2008, Numerical analysis of FGM plate by applying virtual temperature distribution, *7th conference of Iranian aerospace society*, Tehran.